Circadian Rhythm of Redox State Regulates Excitability in Suprachiasmatic Nucleus Neurons

Tongfei A. Wang *et al.*

Science **337**, 839 (2012);
DOI: 10.1126/science.1222826

Science (print ISSN 0036-8075; online ISSN 1095-9203) is published weekly, except the last week in December, by the American Association for the Advancement of Science, 1200 New York Avenue NW, Washington, DC 20005.

30. T. F. Hanisco *et al.*, *J. Phys. Chem. A* **105**, 1543 (2001).
31. E. J. Lanzendorf *et al.*, *J. Phys. Chem. A* **105**, 1535 (2001).
32. D. M. Wilmouth *et al.*, *J. Geophys. Res.* **111**, D16308 (2006).
33. S. P. Sander, *et al.*, *JPL Pub.* **10-6**, 1 (2011).
34. L. T. Molina, M. J. Molina, *J. Phys. Chem.* **91**, 433 (1987).
35. R. J. Salawitch *et al.*, *Geophys. Res. Lett.* **32**, L05811 (2005).
36. A. E. Dessler, *J. Geophys. Res.* **114**, D00H09 (2009).
37. A. E. Dessler, S. C. Sherwood, *J. Geophys. Res.* **109**, D23301 (2004).
38. A. E. Dessler, T. F. Hanisco, S. Fueglistaler, *J. Geophys. Res.* **112**, D18309 (2007).
39. E. R. Keim *et al.*, *Geophys. Res. Lett.* **23**, 3223 (1996).
40. B. F. Thornton *et al.*, *J. Geophys. Res.* **112**, (D18), D18306 (2007).
41. R. J. Trapp, N. S. Diffenbaugh, A. Gluhovsky, *Geophys. Res. Lett.* **36**, L01703 (2009).
42. S. L. Van Klooster, P. J. Roebber, *J. Clim.* **22**, 3317 (2009).
43. L. C. Sloan, D. Pollard, *Geophys. Res. Lett.* **25**, 3517 (1998).
44. D. B. Kirk-Davidoff, E. J. Hintsa, J. G. Anderson, D. W. Keith, *Nature* **402**, 399 (1999).
45. C. Tarnocai *et al.*, *Global Biogeochem. Cycles* **23**, GB2023 (2009).
46. P. J. Crutzen, *Clim. Change* **77**, 211 (2006).
47. D. W. Keith, E. Parson, M. G. Morgan, *Nature* **463**, 426 (2010).
48. M. A. Weinstock, *Environ. Health Perspect.* **103**, (suppl. 8), 251 (1995).
49. T. L. Diepgen, V. Mahler, *Br. J. Dermatol.* **146**, (suppl. 61), 1 (2002).

Acknowledgments: We acknowledge those who have been central to the design of the flight instruments associated with these observations: J. Demusz, N. Allen, C. Tuozzolo, M. Greenberg, M. Rivero, T. Hanisco, J. Paul, L. Moyer, F. Keutsch, and M. Witinski. This research was supported by the NASA Upper Atmosphere Research Program under the technical oversight of K. Jucks.

5 April 2012; accepted 5 July 2012
10.1126/science.1222978

Circadian Rhythm of Redox State Regulates Excitability in Suprachiasmatic Nucleus Neurons

Tongfei A. Wang,[1]* Yanxun V. Yu,[2]*† Gubbi Govindaiah,[1,3] Xiaoying Ye,[3,4]‡ Liana Artinian,[1]§ Todd P. Coleman,[5] Jonathan V. Sweedler,[1,2,3,4] Charles L. Cox,[1,2,3] Martha U. Gillette[1,2,3,6]||

Daily rhythms of mammalian physiology, metabolism, and behavior parallel the day-night cycle. They are orchestrated by a central circadian clock in the brain, the suprachiasmatic nucleus (SCN). Transcription of clock genes is sensitive to metabolic changes in reduction and oxidation (redox); however, circadian cycles in protein oxidation have been reported in anucleate cells, where no transcription occurs. We investigated whether the SCN also expresses redox cycles and how such metabolic oscillations might affect neuronal physiology. We detected self-sustained circadian rhythms of SCN redox state that required the molecular clockwork. The redox oscillation could determine the excitability of SCN neurons through nontranscriptional modulation of multiple potassium (K^+) channels. Thus, dynamic regulation of SCN excitability appears to be closely tied to metabolism that engages the clockwork machinery.

Circadian rhythms coordinate body systems and synchronize the internal milieu with daily and seasonal changes in light on Earth. Diurnal changes in the environment generate daily fluctuations in energy availability, to which internal metabolic systems are tuned by self-sustained circadian clocks (*1*, *2*). These near-24-hour rhythms emerge from transcriptional-translational feedback loops of core clock genes (*3*) and oscillations in regulatory cytoplasmic elements, including adenosine 3′,5′-monophosphate (cAMP) (*4*, *5*), Ca^{2+} (*6*), and activity of protein kinases (*7*). Superimposed upon circadian rhythms of metabolism are near-24-hour oscillations due to the contingencies of life. At the cellular level, metabolic state is manifest as redox state. It is usually described by the homeostasis of reactive free radicals, such as nicotinamide adenine dinucleotide (NAD^+) and flavin adenine dinucleotide (FAD), from reduction-oxidation reactions in metabolism (*8*). Circadian and energetic cycles are coupled through transcriptional modulation by core clock proteins of genes that regulate metabolism (*9*, *10*), as well as the sensitivity of clock gene transcription to redox state (*11*–*13*). However, nontranscriptional interdependency of redox state and neuronal physiology in the circadian context is unexplored.

To determine whether redox state exhibits a daily rhythm in the brain's circadian clock, we performed ratiometric redox fluorometry by two-photon laser microscopy of organotypic slices of suprachiasmatic nucleus (SCN)–bearing rat hypothalamus (*14*). The relative redox state was measured noninvasively from the ratio of autofluorescence emissions in response to 730-nm excitation of two cofactors of cellular metabolism, the oxidized form of FAD (500+ nm) and the reduced form of nicotinamide adenine dinucleotide phosphate (NADPH) (400+ nm) (*15*). We found an endogenous, near-24-hour oscillation of redox state in SCN tissue from wild-type rat and mouse ($\tau = 23.74 \pm 0.26$ (SEM) hours, $\tau = 23.75 \pm 0.30$ hours, respectively; χ^2 periodogram analysis, $N = 5$ brain slices) (Fig. 1, A, B, D, and E). Application of the oxidizing reagent, diamide (DIA, 5 mM), increased the FAD/NADPH ratio within 2 min [$\Delta F_{500+}/F_{400+} = 0.022 \pm 0.018$, $P < 0.05$, paired Student's t test, $N = 6$ brain slices] (fig. S1, A and B). On the other hand, exposure to a reducing reagent, glutathione (GSH, 1 mM), decreased the ratio ($\Delta F_{500+}/F_{400+} = -0.022 \pm 0.010$, $P < 0.01$, paired Student's t test, $N = 6$ brain slices) (fig. S1C). We further evaluated SCN slices from *Bmal1*$^{-/-}$ mice, which lack circadian rhythms (*16*, *17*). *Bmal1*$^{-/-}$ SCNs exhibited stochastic, but not circadian, oscillations in relative redox state (Fig. 1, C and F) ($N = 5$ brain slices). Thus, circadian redox oscillations in rodent SCN require a functional molecular clockwork involving the clock gene, *Bmal1*.

To determine temporal phasing of the SCN redox oscillation, we evaluated two indicators of redox state. First, we examined points across the circadian cycle of SCN brain slices for glutathiolation, the capacity of proteins to incorporate reduced GSH, which binds to available disulfide bonds (*18*). Glutathiolation peaked in the early night, indicating a relatively oxidized state, and was lower in midday, indicating a relatively reduced state (Fig. 1, G and H) [$P < 0.05$, one-way analysis of variance (ANOVA) followed by Tukey's honestly significant difference (HSD) test, $N = 6$ experiments]. We next analyzed the ascorbic acid system, an important antioxidant and neuroprotective buffer in the brain (*19*). We used capillary electrophoresis with laser-induced fluorescence detection (CE-LIF) to directly measure the concentrations of dehydroascorbic acid (DHA) versus its reduced counterpart, ascorbic

[1]Department of Molecular and Integrative Physiology, University of Illinois at Urbana-Champaign, Urbana, IL 61801, USA. [2]Neuroscience Program, University of Illinois at Urbana-Champaign, Urbana, IL 61801, USA. [3]Beckman Institute, University of Illinois at Urbana-Champaign, Urbana, IL 61801, USA. [4]Department of Chemistry, University of Illinois at Urbana-Champaign, Urbana, IL 61801, USA. [5]Department of Bioengineering, University of California, San Diego, La Jolla, CA 92093, USA. [6]Department of Cell and Developmental Biology, University of Illinois at Urbana-Champaign, Urbana, IL 61801, USA.

*These authors contributed equally to this work.
†Present address: Department of Biology and National Center for Behavioral Genomics, Brandeis University, Waltham, MA 02454, USA.
‡Present address: The SAIC-Frederick, Inc., National Cancer Institute, Frederick, MD 21702, USA.
§Present address: Department of Biology, Georgia State University, Atlanta, GA 30302–4010, USA.
||To whom correspondence should be addressed. E-mail: mgillett@illinois.edu

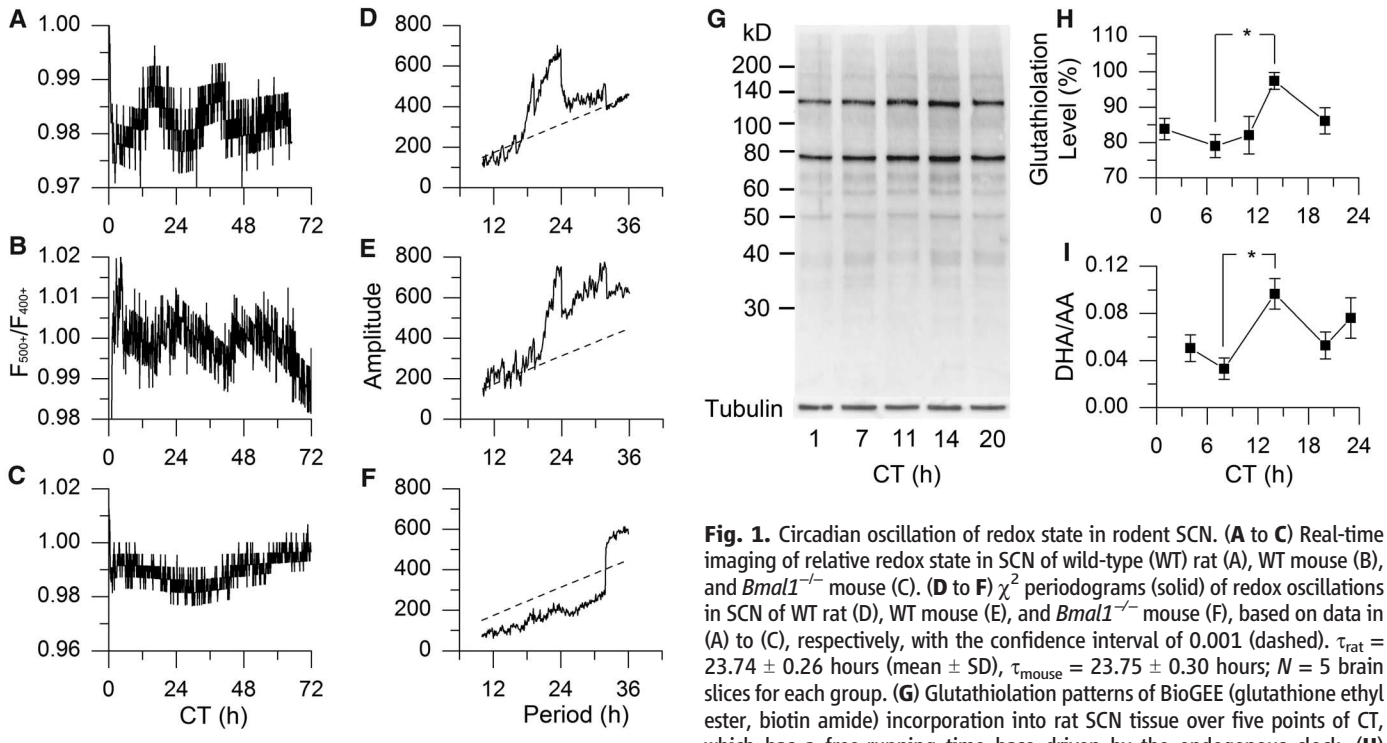

Fig. 1. Circadian oscillation of redox state in rodent SCN. (**A** to **C**) Real-time imaging of relative redox state in SCN of wild-type (WT) rat (A), WT mouse (B), and *Bmal1*$^{-/-}$ mouse (C). (**D** to **F**) χ^2 periodograms (solid) of redox oscillations in SCN of WT rat (D), WT mouse (E), and *Bmal1*$^{-/-}$ mouse (F), based on data in (A) to (C), respectively, with the confidence interval of 0.001 (dashed). τ_{rat} = 23.74 ± 0.26 hours (mean ± SD), τ_{mouse} = 23.75 ± 0.30 hours; N = 5 brain slices for each group. (**G**) Glutathiolation patterns of BioGEE (glutathione ethyl ester, biotin amide) incorporation into rat SCN tissue over five points of CT, which has a free-running time base driven by the endogenous clock. (**H**) Protein glutathiolation over five CTs in rat SCN (P < 0.05, one-way ANOVA; *, P < 0.05, Tukey's HSD test; N = 6 experiments on separate SCNs). (**I**) DHA/AA ratio in rat SCN over five CTs (P < 0.05, one-way ANOVA; *, P < 0.05, Tukey's HSD test; N = 3 experiments on separate SCNs).

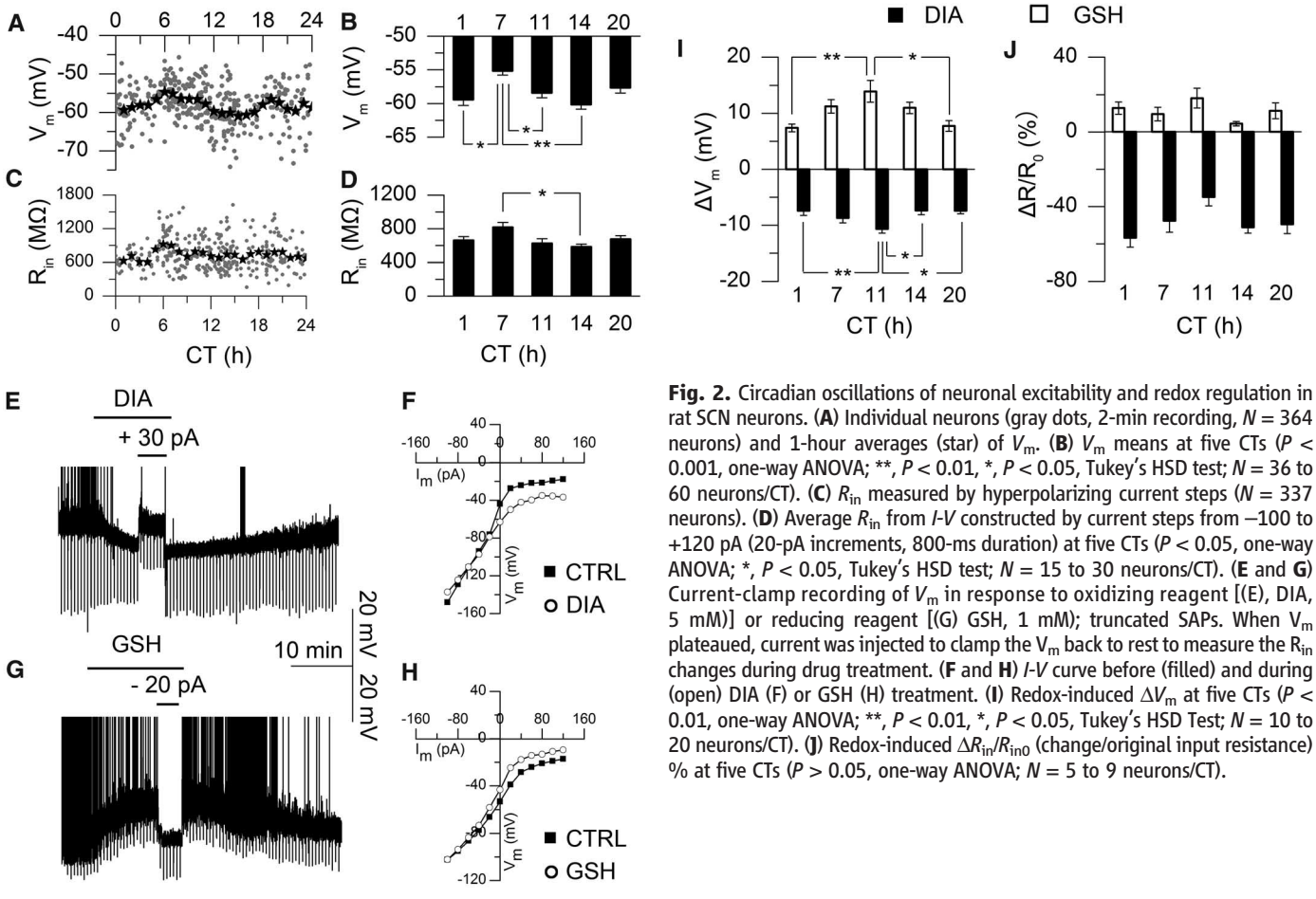

Fig. 2. Circadian oscillations of neuronal excitability and redox regulation in rat SCN neurons. (**A**) Individual neurons (gray dots, 2-min recording, N = 364 neurons) and 1-hour averages (star) of V_m. (**B**) V_m means at five CTs (P < 0.001, one-way ANOVA; **, P < 0.01, *, P < 0.05, Tukey's HSD test; N = 36 to 60 neurons/CT). (**C**) R_{in} measured by hyperpolarizing current steps (N = 337 neurons). (**D**) Average R_{in} from I-V constructed by current steps from −100 to +120 pA (20-pA increments, 800-ms duration) at five CTs (P < 0.05, one-way ANOVA; *, P < 0.05, Tukey's HSD test; N = 15 to 30 neurons/CT). (**E** and **G**) Current-clamp recording of V_m in response to oxidizing reagent [(E), DIA, 5 mM)] or reducing reagent [(G) GSH, 1 mM); truncated SAPs. When V_m plateaued, current was injected to clamp the V_m back to rest to measure the R_{in} changes during drug treatment. (**F** and **H**) I-V curve before (filled) and during (open) DIA (F) or GSH (H) treatment. (**I**) Redox-induced ΔV_m at five CTs (P < 0.01, one-way ANOVA; **, P < 0.01, *, P < 0.05, Tukey's HSD Test; N = 10 to 20 neurons/CT). (**J**) Redox-induced $\Delta R_{in}/R_{in0}$ (change/original input resistance) % at five CTs (P > 0.05, one-way ANOVA; N = 5 to 9 neurons/CT).

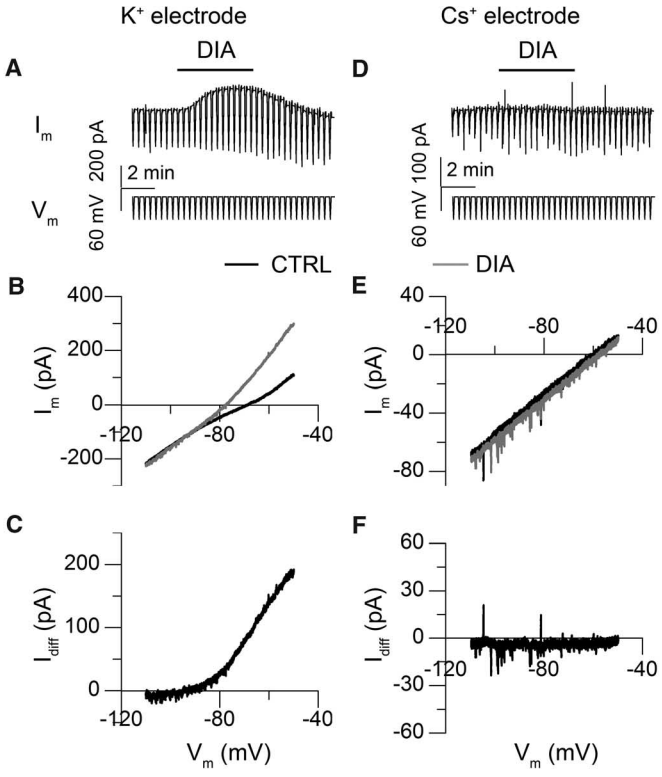

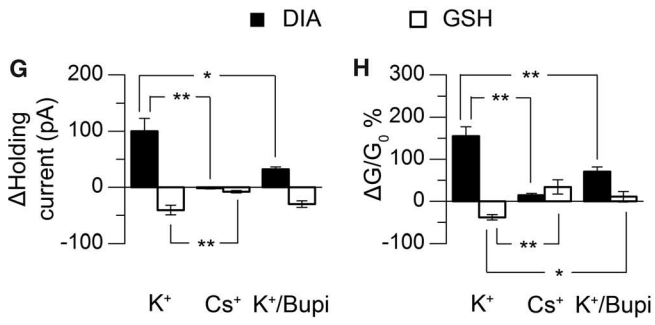

Fig. 3. Redox regulation of neuronal excitability through K^+ current (CT 9 to 13 hours). (**A**) Voltage-clamp recording of SCN neuron, with repeating slow-ramped voltage commands from −50 mV to −110 mV. (**B**) *I-V* curve constructed based on the command voltage and membrane current recorded, before (black) and during (gray) DIA treatment. (**C**) The DIA-evoked current as calculated from the difference in the membrane response in (B). (**D** to **F**) Similar voltage-clamp recordings as (A) to (C), respectively, except that Cs^+ replaced K^+ in the patch pipette. (**G** and **H**) Holding current (G) and conductance (H) changes induced by redox reagents (DIA, black; GSH, white) with electrodes containing K^+ ($P < 0.01$, paired Student's *t* test to control; $N = 6$ neurons), Cs^+ [$P > 0.05$ (current), $P < 0.01$ (conductance) for DIA, $P < 0.05$ for GSH, paired Student's *t* test to control; $N = 6$ neurons], or K^+ (in electrode) with bupivacaine (Bupi, 100 μM) in bath ($P < 0.01$, paired Student's *t* test to control; $N = 5$ neurons); for the comparison across groups, $P < 0.01$, one-way ANOVA; **, $P < 0.01$, *, $P < 0.05$, Tukey's HSD test.

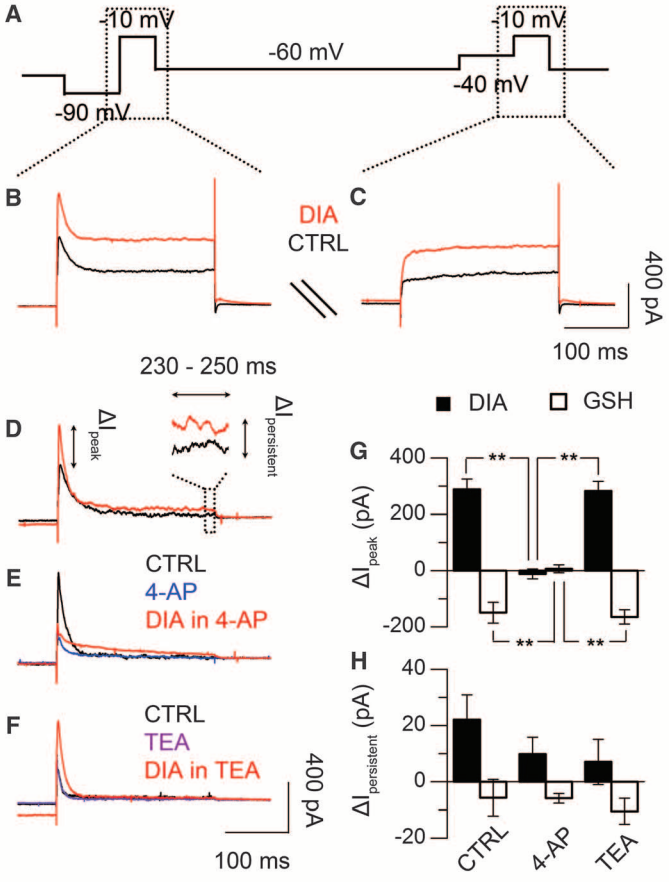

Fig. 4. Redox regulation of voltage-dependent K^+ currents (CT 9 to 13 hours). (**A**) Recording protocol of repeating voltage-step commands to voltage-clamped SCN neurons (*15*), before, during, and after drug treatment. (**B** and **C**) Current responses to the voltage-step commands of −10 mV pulses, after either −90 mV (B) or −40 mV (C) prepulse, before (black) or during (red) DIA treatment. (**D**) Voltage-dependent outward current in response to −10 mV voltage-step stimulation, calculated from the difference between the current responses in (B) and (C). (**E** and **F**) Effects of 4-AP (5 mM) and TEA (20 mM) on outward current evoked by DIA. (**G**) Transient current (<10 ms) changes in response to redox treatment (DIA, black; GSH, white), with or without 4-AP or TEA ($P < 0.01$, one-way ANOVA; **, $P < 0.01$, Tukey's HSD test; $N = 5$ to 6 neurons/condition). (**H**) Persistent current (230 to 250 ms) changes in response to redox treatment, with or without 4-AP or TEA ($P > 0.05$, one-way ANOVA; $N = 5$ to 6 neurons/condition).

acid (AA) (*20*). Amounts of DHA/AA oscillate with a circadian rhythm, similar to glutathiolation: DHA/AA is highest in the early night and lowest in midday (Fig. 1I) ($P < 0.05$, test as above, $N = 3$ experiments). Parallel changes in these distinct redox systems confirm circadian oscillation of global redox state in rat SCN, with a significantly oxidized state in the early night versus a reduced state during the daytime. These results support and extend the redox oscillation found in peripheral tissue (*21*, *22*) to the central circadian clock in the brain.

To assess possible relations between the circadian oscillations of redox state and neuronal physiology, we evaluated membrane excitability in rat SCN neurons by examining resting membrane potential (V_m), input resistance (R_{in}), and spontaneous action potentials (SAP). Recording from current-clamped neurons, we observed circadian oscillations of V_m [Fig. 2A, $N = 364$ neurons; Fig. 2B, $N = 36$ to 60 neurons/CT at five circadian times (CTs) around the free-running clock cycle, $P < 0.001$, test as above], R_{in} (Fig. 2C, $N = 337$ neurons; Fig. 2D, $N = 15$ to 30 neurons/CT, $P < 0.05$, test as above), frequency of SAP (fig. S2A, $N = 334$ neurons), and percentage of neurons discharging SAP (active, fig. S2C, $N = 334$ neurons) (*15*). These data from rats exhibit a similar circadian pattern in membrane excitability as from mice (*23*). Comparing circadian oscillations of redox state (Fig. 1, H and I) with V_m in SCN neurons (Fig. 2B) revealed that the daytime reduced state matched the depolarized V_m, whereas the oxidized state of subjective night aligned with hyperpolarized V_m.

To probe potential interdependency of redox state and neuronal excitability, we tested the effects of pharmacological redox manipulation on V_m of SCN neurons at various CTs. The oxidizing reagent, DIA, hyperpolarized V_m in a reversible manner (Fig. 2E, –8.68 ± 0.64 mV, mean around circadian cycle, N = 104 neurons); in contrast, exposure to the reducing reagent, GSH, caused depolarization (Fig. 2G, +10.67 ± 1.03 mV, N = 97 neurons). Similar results were obtained from current-clamp recording with redox reagents in the patch pipette (fig. S4). Exogenous redox regulation of V_m in SCN depends on CT: both drugs caused maximal effects near subjective dusk (CT 10 to 12 hours) and minimal effects near subjective dawn (CT 0 to 2 hours, Fig. 2I, $P < 0.01$, test as above, N = 10 to 20 neurons/CT). Shifts in V_m caused by redox manipulation were associated with changes of R_{in}. Based on the slopes of current-voltage (*I-V*) curves constructed before and during redox treatment, DIA was found to decrease the R_{in} of SCN neurons by 364 ± 30 MΩ (48.83%, Fig. 2, F and J, N = 41 neurons), whereas GSH increased R_{in} by 64 ± 11 MΩ (10.81%, Fig. 2, H and J, N = 36 neurons). Percentage changes in R_{in} were not correlated with changes in V_m (fig. S5, $P > 0.05$, linear correlation and regression, N = 37 to 42 neurons) and were independent of CT (Fig. 2J, $P > 0.05$, one-way ANOVA, N = 5 to 9 neurons/CT). Redox-induced changes in membrane properties were rapid, occurring in <2 min (68.7 ± 10.6 s).

To identify potential targets for redox regulation of neuronal excitability, we gradually changed command voltages from –50 to –110 mV (6-s duration) on voltage-clamped SCN neurons between CT 9 and 13 hours. By comparing membrane currents before and during exposure to the redox reagents, we examined the voltage dependency of target ion channels. Bath application of DIA elicited a strong outward current (100.1 ± 22.8 pA at –50 mV, N = 6 neurons) (Fig. 3, A, B, C, and G), associated with an increased conductance as indicated by a greater slope of the current response to the ramped voltage command. The *I-V* relationship before and during DIA treatment revealed a reversal potential at –81.4 ± 7.0 mV and conductance increases of 154.9 ± 22.5% (Fig. 3, B and H). Thus, DIA appears to act through an outward-rectifier K^+ channel (Fig. 3C). We confirmed this prediction by replacing K^+ with Cs^+, a general K^+-channel blocker, in the recording pipette. Under this condition, the DIA-evoked outward current was significantly attenuated (–1.6 ± 1.2 pA at –50 mV, $P < 0.01$, Tukey's HSD Test, N = 6 neurons) (Fig. 3, D to G). Only small conductance changes could be detected during DIA treatment (14.2 ± 4.7%) (Fig. 3, E and H). Exposure to GSH elicited an inward current in SCN neurons (–40.6 ± 8.5 pA at –50 mV, N = 6 neurons/condition) (Fig. 3G), with a reversal potential at –79.9 ± 4.0 mV and a conductance change of –38.2 ± 6.3% (Fig. 3H). The GSH-evoked inward current was attenuated by Cs^+ in the internal solution, as well (–7.9 ± 2.1 pA at –50 mV, 34.1 ± 16.8% conductance changes, $P < 0.01$, test as above, N = 6 neurons/condition) (Fig. 3, G and H), also supporting the involvement of K^+ currents.

To explore the potential role of leak K^+ channels in redox regulation, we applied a specific blocker of this channel, bupivacaine (Bupi, 100 μM). In the presence of Bupi, DIA induced an outward current of 31.9 ± 4.4 pA at –50 mV (Fig. 3G) (N = 5 neurons/condition), with conductance changes of 70.4 ± 11.2% (Fig. 3H) (N = 5 neurons), but amplitudes were lower than those in control media (Fig. 3, G and H) ($P < 0.05$, test as above). Bupi attenuated GSH-induced inward current and conductance changes, as well (–40.6 ± 8.5 pA at –50 mV, 11.0 ± 12.4%, $P < 0.05$, test as above, N = 5 neurons/condition) (Fig. 3, G and H). These results support the leak K^+ channel as a target of redox regulation.

We further used voltage-step commands to examine the possibility that redox state regulates voltage-gated K^+ channels (Fig. 4, A to C) (*15*). We found that DIA significantly enhanced the transient peak of the outward current induced by –10 mV steps (288.4 ± 36.5 pA, N = 5 neurons) (Fig. 4, D and G). This enhancement was completely abolished by 4-aminopyridine (4-AP, 5 mM), a selective inhibitor of A-type K^+ channel (–11.7 ± 17.2 pA, $P < 0.01$, test as above, N = 6 neurons) (Fig. 4, E and G), but was insensitive to tetraethylammonium (TEA, 20 mM), a delayed rectifier K^+-channel blocker (282.4 ± 34.7 pA, $P > 0.05$, test as above, N = 6 neurons) (Fig. 4, F and G). The persistent outward current was insensitive to DIA treatment with or without 4-AP or TEA ($P > 0.05$, one-way ANOVA, N = 5 to 6 neurons) (Fig. 4H). On the other hand, GSH suppressed the transient peak of the outward current (–149.5 ± 37.3 pA, N = 5 neurons) (Fig. 4G); similar to DIA, the suppression was sensitive to 4-AP (6.8 ± 14.3 pA, $P < 0.01$, Tukey's HSD Test, N = 5 neurons) (Fig. 4G) but not TEA (–164.8 ± 25.4 pA, $P > 0.05$, test as above, N = 6 neurons) (Fig. 4G), whereas the persistent outward current was not affected by any drug ($P > 0.05$, one-way ANOVA, N = 5 to 6 neurons/condition) (Fig. 4H). These results support the involvement of a 4-AP–sensitive voltage-gated K^+ channel in redox regulation.

The daily rhythm of electrical activity in the SCN is essential for the functionality of the central pacemaker in synchronizing the body clocks (*24*, *25*); several K^+ channels have been identified underlying the changing excitability (*26*–*28*). We found that a redox regulation of K^+ conductance underwent circadian changes in SCN neurons, with characteristics of both leak and A-type K^+ channels. This provides a nontranscriptional pathway for the metabolic cycle to engage the clockwork machinery (fig. S6). Energetic fluctuation in the central nervous system has been considered to be a consequence of neuronal activity. However, our study implies that changes in cellular metabolic state could be the cause, rather than the result, of neuronal activity. Cross talk between energetic and neuronal states bridges cellular state to systems physiology.

References and Notes

1. C. B. Green, J. S. Takahashi, J. Bass, *Cell* **134**, 728 (2008).
2. J. Bass, J. S. Takahashi, *Science* **330**, 1349 (2010).
3. P. L. Lowrey, J. S. Takahashi, *Annu. Rev. Genomics Hum. Genet.* **5**, 407 (2004).
4. R. A. Prosser, M. U. Gillette, *Brain Res.* **568**, 185 (1991).
5. J. S. O'Neill, E. S. Maywood, J. E. Chesham, J. S. Takahashi, M. H. Hastings, *Science* **320**, 949 (2008).
6. M. C. Harrisingh, Y. Wu, G. A. Lnenicka, M. N. Nitabach, *J. Neurosci.* **27**, 12489 (2007).
7. M. S. Robles, C. Boyault, D. Knutti, K. Padmanabhan, C. J. Weitz, *Science* **327**, 463 (2010).
8. W. Dröge, *Physiol. Rev.* **82**, 47 (2002).
9. F. W. Turek *et al.*, *Science* **308**, 1043 (2005).
10. B. Marcheva *et al.*, *Nature* **466**, 627 (2010).
11. J. Rutter, M. Reick, L. C. Wu, S. L. McKnight, *Science* **293**, 510 (2001).
12. E. M. Dioum *et al.*, *Science* **298**, 2385 (2002).
13. J. Rutter, M. Reick, S. L. McKnight, *Annu. Rev. Biochem.* **71**, 307 (2002).
14. S. Huang, A. A. Heikal, W. W. Webb, *Biophys. J.* **82**, 2811 (2002).
15. Materials and methods, supplementary text, and supplementary figures are available as supplementary materials on *Science* Online.
16. M. K. Bunger *et al.*, *Cell* **103**, 1009 (2000).
17. C. H. Ko *et al.*, *PLoS Biol.* **8**, e1000513 (2010).
18. D. M. Sullivan, R. L. Levine, T. Finkel, *Methods Enzymol.* **353**, 101 (2002).
19. M. E. Rice, *Trends Neurosci.* **23**, 209 (2000).
20. W. S. Kim, R. L. Dahlgren, L. L. Moroz, J. V. Sweedler, *Anal. Chem.* **74**, 5614 (2002).
21. J. S. O'Neill, A. B. Reddy, *Nature* **469**, 498 (2011).
22. J. S. O'Neill *et al.*, *Nature* **469**, 554 (2011).
23. M. D. Belle, C. O. Diekman, D. B. Forger, H. D. Piggins, *Science* **326**, 281 (2009).
24. T. M. Brown, H. D. Piggins, *Prog. Neurobiol.* **82**, 229 (2007).
25. D. A. Golombek, R. E. Rosenstein, *Physiol. Rev.* **90**, 1063 (2010).
26. J. N. Itri, S. Michel, M. J. Vansteensel, J. H. Meijer, C. S. Colwell, *Nat. Neurosci.* **8**, 650 (2005).
27. M. De Jeu, A. Geurtsen, C. Pennartz, *J. Neurophysiol.* **88**, 869 (2002).
28. J. N. Itri *et al.*, *J. Neurophysiol.* **103**, 632 (2010).

Acknowledgments: We thank S.-H. Tyan for insightful discussions at the inception of this work; G. Robinson, R. Gillette, and J. M. Mitchell for critical feedback; J. M. Ding and G. F. Buchanan for data support; K. E. Weis and J. M. Arnold for technical support; S. C. Liu for data analysis consultation; and M. C. Holtz for manuscript preparation. Research was supported by the National Heart, Lung, and Blood Institute (RO1HL092571 Z ARRA, RO1HL086870) to M.U.G., the National Eye Institute (EY014024) to C.L.C., the National Institute on Drug Abuse (P30DA018310) to J.V.S., and the National Science Foundation (CHE 11-11705 to J.V.S. and CCF09-39370 to T.P.C.). Content is solely the responsibility of the authors and does not necessarily represent the official views of NIH or NSF.

Supplementary Materials

www.sciencemag.org/cgi/content/full/science.1222826/DC1
Materials and Methods
Supplementary Text
Figs. S1 to S6
References (*29*–*44*)

3 April 2012; accepted 29 June 2012
Published online 2 August 2012;
10.1126/science.1222826